ISSN 2288-8403(Online)

한국표면공학회지
J. Surf. Sci. Eng.
Vol.56, No.6, 2023.
https://doi.org/10.5695/JSSE.2023.56.6.393

〈Research Article〉

Synthesis of Ce-doped In_2O_3 nanoparticles via a microwave-assisted hydrothermal pathway and their application as an ultrafast breath acetone sensor

Byeong-Hun Yu[a], Sung Do Yun[b], Chan Woong Na[b,*], Ji-Wook Yoon[a,*]

[a]Department of Electronic and Information Materials Engineering, Division of Advanced Materials Engineering, Jeonbuk National University, Jeonju Baekjaedaero 567, Korea
[b]Dongnam Division, Korea Institute of Industrial Technology, Busan Baegyang-daero 804, Korea

(Received 07 November, 2023 ; revised 19 December, 2023 ; accepted 21 December, 2023)

Abstract

Acetone, a metabolite detected from the exhaled breath of people doing a diet, can be used for non-invasive monitoring of diet efficiency. Thus, gas sensors with rapid response and recovery characteristics to acetone need to be developed. Herein, we report ultrafast acetone sensors using Ce-doped In_2O_3 nanoparticles prepared by the one-pot microwave-assisted hydrothermal method. The pure In_2O_3 sensor shows a high response and fast response time (τ_{res} = 6 s) upon exposure to 2 ppm acetone at 300 ℃, while exhibiting a relatively sluggish recovery speed (τ_{recov} = 1129 s). When 20 wt% Ce is doped, the τ_{recov} of the sensor significantly decreased to 45 s withholding the fast-responding characteristic (τ_{res} = 6 s). In addition, the acetone response (resistance ratio, S) of the sensor is as high as 5.8, sufficiently high to detect breath acetone. Moreover, the sensor shows similar acetone sensing characteristics even under a highly humid condition (relative humidity of 60%) in terms of τ_{res} (6 s), τ_{recov} (47 s), and S (4.7), demonstrating its high potential in real applications. The excellent acetone sensing characteristics of Ce-doped In_2O_3 nanoparticles are discussed in terms of their size, composition, phase, and oxygen adsorption on the sensing surface.

Keywords : Gas sensor; acetone; fast recovery; Ce-In_2O_3; microwave-assisted hydrothermal synthesis.

1. Introduction

Obesity is a severe disease that increases the risk of high blood pressure, diabetes, hyperlipidemia, and even cancer (in particular, liver, pancreas, and gastroesophageal). To avoid contracting such diseases, obese must try to lose weight via proper dieting methods. A ketogenic diet (KD), reducing carbohydrate intake to ~50 g day-1, is one of the proven remedies to lose weight, scientifically. The KD promotes body fat burn by catabolizing the fat into three different ketone bodies, which are acetoacetate, β-hydroxyl butyrate, and acetone [1]. Thus, monitoring such metabolites is a proper way to confirm the efficiency of dieting methods.

Among the metabolites, only acetone is in the gas phase, hence observed from exhaled breath. It has been reported that the concentration of breath acetone is closely related to fat burn rates during diets. For instance, breath acetone levels become raised to 2–5 ppm when the body fat decomposition

*Corresponding Author : Ji-Wook Yoon, Chan Woong Na
Jeonbuk National University, Korea Institute of Materials Science
E-mail: jwyoon@jbnu.ac.kr,cwna@kitech.re.kr

rate reaches 2 g h^{-1} [1]. Considering this fact, breath acetone analysis is a non-invasive and convenient tool to guide obese to lose their weight effectively. This method could enable routine assessment if performed using chemosensors being cost-effective and portable [2]. Thus, developing chemosensors for breath acetone monitoring is in high demand.

Oxide semiconductor gas sensors have been extensively explored in detecting breath acetone due to their high sensitivity, simple structure, and cost-effectiveness. In particular, oxide semiconductors such as SnO_2 [3], NiO [4], ZnO [5], and In_2O_3 have been mainly studied, as they are sensitive to acetone [6]. The sensors using the materials above have demonstrated acetone detection even at ppm levels if nanostructured [7]. Among these, In_2O_3 nanostructures, a wide bandgap semiconductor with high surface-to-volume ratios, have shown a high potential to detect low concentrations of acetone [8]. The acetone response can be further enhanced by loading or doping catalysts, providing improved surface reaction between the acetone and the sensing surface [9]. Karmaoui et al. [10] reported that Pt-decorated In_2O_3nanoparticles could detect acetone even at ppb levels (< 10 ppb).

However, other key features such as response and recovery properties should be also considered for designing high-performance breath acetone sensors. Fast response time is crucial, considering that human generally cannot deliver their breath to sensors for more than several tens of seconds. Recovery speed is also very important for consecutive uses of the sensors in a short time. Yoon et al. [11] reported that the response and recovery times of In_2O_3 nanostructures (i.e., In_2O_3 hollow spheres) can be drastically reduced if Ce exists on their surface. Although the sensors demonstrated fast response and recovery kinetics, the synthetic method was too complicated, as the forming of surface Ce was accomplished via multiple layer-by-layer assemblies. Thus, to boost the potential of Ce-In_2O_3 in breath acetone detection, what we urgently need is a new strategy for the facile and simple preparation of Ce-In_2O_3nanostructures.

Herein, we report a facile synthesis of Ce-doped In_2O_3 nanoparticles and their ultrafast responding/recovering properties to acetone. The nanoparticles were prepared by a one-pot microwave-assisted hydrothermal method, and the Ce-doping concentration was controlled in the range of 0–50 wt%. The sensor prepared using the pure In_2O_3 nanoparticles showed a high response and fast response speed to acetone while showing sluggish recovery kinetics for more than 18 minutes. On the other hand, when 20% of Ce was doped, the sensor showed a much-reduced recovery speed, along with sufficiently high response and fast response characteristics. The sensor maintained excellent acetone sensing properties even under highly humid conditions (e.g., relative humidity (RH) = 60%), demonstrating its potential for the rapid detection of acetone in human breath. In this paper, the excellent acetone sensing performance was discussed from the viewpoints of the particle size, the crystal structure, the composition, and the oxygen adsorption on the sensing surface.

2. Experimental

2.1 Preparation of Ce-doped In_2O_3 nanoparticles

Ce-doped In_2O_3 nanoparticles were synthesized by microwave-assisted hydrothermal and subsequent thermal annealing. First, 1.15g of indium (III) chloride ($InCl_3$, 98%, Sigma-Aldrich) and 0-50 wt% of Ce nitrate hexahydrate ($Ce(NO_3)_3{\cdot}6H_2O$,

distilled water. The homogeneous solution was transferred to a microwave oven (Mars 5, CEM) and heated to a reaction temperature of 180 ℃ within 5 min. The temperature remained for 1 h. After that, the suspension was cooled down and washed/centrifuged five times with distilled water. The precursors for Ce-doped In_2O_3 nanoparticles were obtained by drying the suspension at 60 ℃ for 12 h, followed by annealing at 500 ℃ for 4 h in air. For simplicity, the In_2O_3 nanoparticles doped with 10, 20, and 50 wt% of Ce are referred to as '10Ce-In_2O_3', '20Ce-In_2O_3', and '50Ce-In_2O_3', respectively.

2.2 Characterization

The morphologies of the nanoparticles were observed by field emission-scanning electron microscopy (FE-SEM, Gemini500, Carl Zeiss) and transmission electron microscopy (TEM, ARM200F, JEOL). The crystal structure of the nanoparticles was analyzed by X-ray diffraction (XRD, LabX XRD-6100, Shimadzu).

2.3 Fabrication of Ce-doped In_2O_3 sensors

A slurry was prepared by dispersing the Ce-doped In_2O_3 nanoparticles in distilled water. The sensor was fabricated by drop-coating the slurry onto an alumina sensor substrate with Au electrodes on the top and a Ru micro-heater on the bottom. Before the measurement, the sensor was heat-treated at 500 ℃ for 2 h to remove residual impurities.

2.4 Gas sensing test

The gas sensing properties of the prepared sensors were evaluated in a quartz chamber coupled with a gas supply system. This system controls the atmosphere in the chamber by changing the mixing ratio between dry synthetic air and analyte gases (5 ppm acetone, carbon monoxide, ammonia, ethylene, nitrogen dioxide) using mass flow controllers. The level of relative humidity (RH) in the chamber was controlled by admixing humid air generated by bubbling distilled water. The total flow was fixed at 200 mL min^{-1}. The DC resistance of the sensors was monitored using a picoammeter (6487, Keithley Co., Ltd.) interfaced with a computer. The gas response (S) was calculated as R_a/R_g, where R_g is the sensor resistance in an analyte gas and R_a is the sensor resistance in air. The 90% response time (τ_{res}) and recovery time (τ_{recov}) were defined as the time to reach a 90% resistance change upon exposure to the analytic gas and air, respectively.

3. Results

XRD patterns for the pure In_2O_3 and Ce-doped In_2O_3 nanoparticles are shown in Figure 1. The pure In_2O_3 nanoparticles exhibited a rhombohedral phase (JCPDS #21-0406). This may be unusual given that the crystal structures of In_2O_3 reported in the literature are mostly cubic [12]. However, this is possible considering that microwave irradiation generally promotes the formation of InOOH, a precursor for rhombohedral In_2O_3 while hindering the formation of $In(OH)_3$, a precursor for cubic In_2O_3 [13]. Thus, the formation of rhombohedral In_2O_3in the present study can be explained by the fact that the nanoparticles were prepared by microwave-assisted hydrothermal. Note that one of the authors has demonstrated the facile preparation of rhombohedral In_2O_3nanoparticles via the microwave-assisted hydrothermal pathway [14].

In the case of In_2O_3 with 0–20 wt% of Ce, no second phase related to Ce was found (Fig. 1a1-c1). Instead, low-angle shifts of the main peak of In_2O_3 with increasing amounts of Ce (0, 10, and 20 wt%) were observed, shifting from 31.02°to 30.99° and 30.95°, respectively

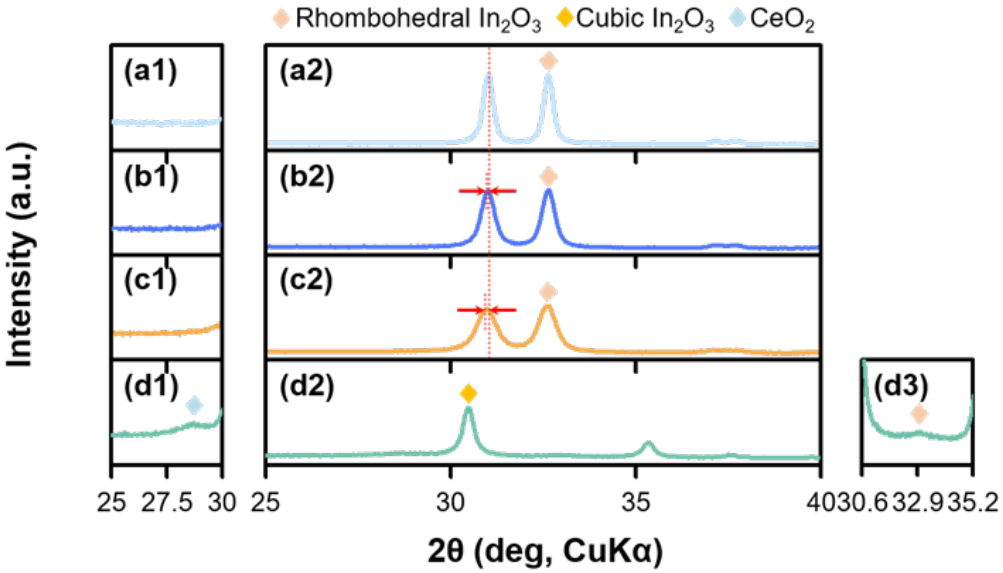

Fig. 1 XRD patterns of (a1-2) pure In_2O_3, (b1-2) 10Ce-In_2O_3, (c1-2) 20Ce-In_2O_3, and (d1-3) 50Ce-In_2O_3.

(Fig.1a2-c2). This suggests that added Ce was substitutionally incorporated into the lattice of the In_2O_3. Note that the ionic radius of Ce^{4+} (0.87 Å) at the coordination number (CN) of 6 is slightly larger than that of In^{3+} (0.80 Å) at the same CN, enabling such peak shifts. When the Ce concentration increased to 50 wt%, a CeO_2 peak started to be found at 28.71° (Fig. 1d1). This indicates that the excessive Ce over the solubility limit turned into cubic CeO_2 (JCPDS #004-0593). At the same time, the phase of as-prepared samples change from the rhombohedral In_2O_3 with the main peak of 32.99° to the cubic In_2O_3 (JCPDS #06-0416) which primary peak located at 30.48°(Fig. 1d2-d3). This implies that the formation of the hetero-interface between CeO_2 and In_2O_3facilitated the transformation of the phase of In_2O_3 from rhombohedral to cubic. This phase transformation might occur to reduce crystal structure mismatch between rhombohedral In_2O_3 and cubic CeO_2. This suggests that the maximum amount of Ce that can be doped into In_2O_3 without damaging its rhombohedral structure is <50 wt%.

The crystallite sizes of the particles (dXRD) calculated by Scherrer's equation were 24, 21, 16, and 19 nm for pure In_2O_3, 10Ce-In_2O_3, 20Ce-In_2O_3, and 50Ce-In_2O_3, respectively. The dXRD decreased at the Ce concentration of 0–20 wt% while increasing again at 50 wt%, which also supports that the Ce below 20 wt% was doped into the In_2O_3 lattice. In addition, this shows that the 20Ce-In_2O_3 nanoparticles possessed the smallest crystallite size among the samples.

The SEM images of the pure and Ce-doped In_2O_3 nanoparticles are shown in Figure 2a1-d1. For pure In_2O_3, the particles exhibited an agglomerated form of a few tens of nanoparticles (Fig. 2a1). The mean size of the diameter of agglomerates was ~150 nm. For Ce-doped samples, the size of agglomerates decreased as the concentration of Ce-doping increased, ultimately reaching approximately 90 nm when the Ce concentration reached 20 wt%. (Fig. 2b1,c1). However, when Ce concentration increased to 50 wt%, the size of agglomerates increased again to >200 nm (Fig. 2d1). From the SEM images, the primary particle size seemed to constantly decrease with increasing Ce doping concentrations, unlike the result from Scherrer's equation. To clarify this, TEM observation was conducted (Fig. 2a2-d2). The images

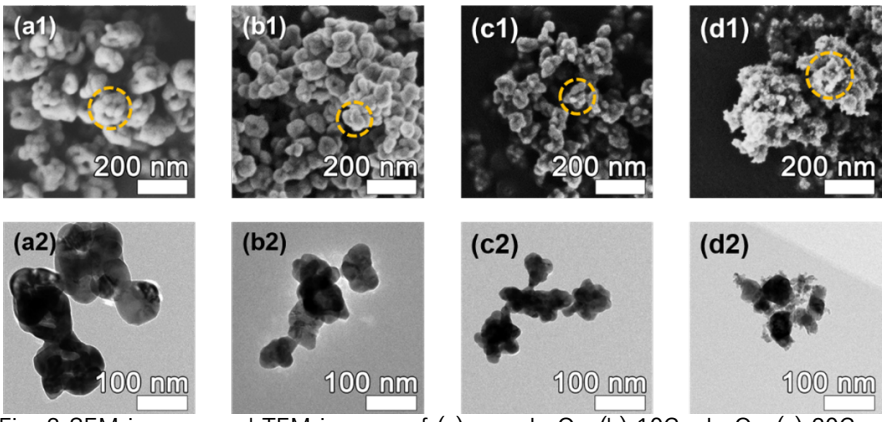

Fig. 2 SEM images and TEM images of (a) pure In_2O_3, (b) 10Ce-In_2O_3, (c) 20Ce-In_2O_3, and (d) 50Ce-In_2O_3.

confirmed that the primary particle size of Ce-doped In_2O_3 was similar to the values from Scherrer's equation. In addition, the small nanoparticles in the SEM image of the 50Ce-In_2O_3 sample were revealed to be several nanometer-sized CeO_2 nanoparticles (Fig. 2d2). The existence of ultrafine CeO_2 nanoparticles can explain the increase in the size of agglomerates. This is because smaller nanoparticles are more readily agglomerated than larger particles. Considering this fact, the increase in the size of agglomerates of the 50Ce-In_2O_3 can be understood by the facilitated agglomeration between the In_2O_3 nanoparticles due to ultrafine CeO_2 nanoparticles. This indicates that the existence of CeO_2 nanoparticles is not favorable for acquiring less agglomerated structures.

The gas sensing properties of the pure In_2O_3 and Ce-doped In_2O_3 sensors were evaluated (Figure. 3). The pure In_2O_3 sensor showed a bell-shape response curve to 2 ppm acetone at 300–400℃ and exhibited the highest acetone response at 350℃ (Fig. 3a). At 350℃, the acetone response was 22.9. As soon as Ce was doped, the acetone response was decreased (Fig. 3b). The acetone response and Ce doping concentration showed an inversely proportional relationship. This is due to the increase in the gas-insensitive Ce on the In_2O_3 sensing surface and corresponds to the result in the literature [11]. Nevertheless, even with the high Ce doping concentration of 50 wt%, the sensor showed a high gas response (2.3) to 2 ppm acetone. This is possibly due to the small crystallite sizes at a few ten-nanometer scales and the rhombohedral phase of In_2O_3. Note that small crystallite sizes can maximize the chemo-resistive variation of the particles [15], and the rhombohedral In_2O_3 is known to exhibit a higher response to gases than the cubic In_2O_3 due to its high electrical conductivity and (104) plane

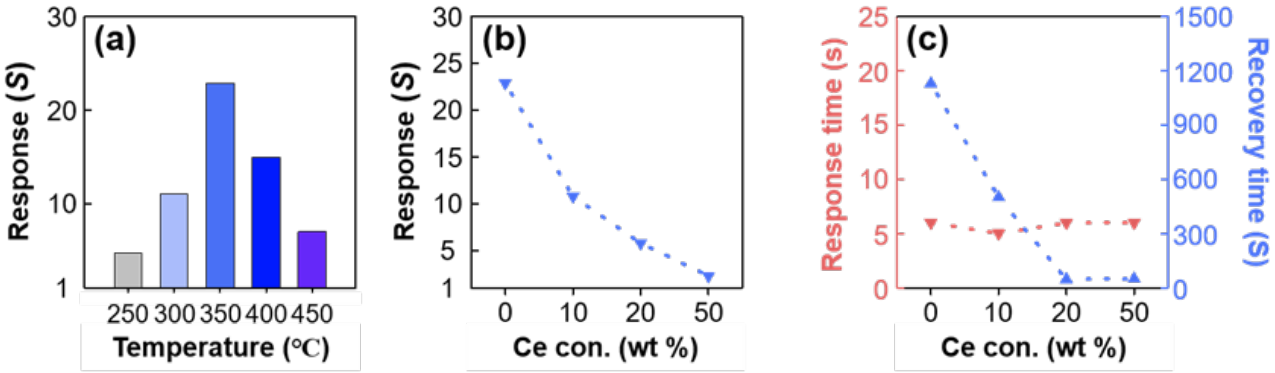

Fig. 3 (a) Gas responses of pure In_2O_3 sensor to 2 ppm acetone at 250–450 ℃, (b) gas responses of pure In_2O_3 and Ce-doped In_2O_3 nanoparticle sensors to 2 ppm acetone at 350 ℃, (c) response/recovery times of the sensors to 2 ppm acetone at 350 ℃

that is favorable for gas adsorption [14]. This indicates that both pure In_2O_3 and Ce-doped In_2O_3 nanoparticles are excellent platform materials, in terms of gas response, for detecting the breath acetone of dieting people.

The τ_{res} of the pure In_2O_3 sensor was fast as 6 s, which also remained in the Ce-doped In_2O_3 sensors (5–6 s) regardless of Ce doping concentrations (Fig. 3c). This indicates that all the sensors in the present work can detect breath acetone in a sufficiently fast manner. However, in terms of τ_{recov}, the pure In_2O_3 sensor exhibited sluggish recovery speed (Fig. 3c). The τ_{recov} was 1129 s, representing that the sensor needs more than 18 min waiting time for repetitive use. On the other hand, the Ce-doped In_2O_3 sensors showed significantly enhanced recovery characteristics. The τ_{recov} constantly decreased with increasing Ce doping concentration and reduced even to 47 s at the Ce doping concentration of 20 wt%. This suggests that Ce doping significantly enhanced the recovery characteristics of the In_2O_3 sensors. In general, one of the key processes for the recovery of oxide semiconductor sensors is the re-adsorption of oxygen ions on the sensing surface [16], and Cerium oxide is known to possess higher oxygen adsorption ability compared with other oxides [17]. This suggests that the ultrafast recovery speed of the Ce-doped In_2O_3 sensors emanated from the enhanced oxygen adsorption on the sensing surface via Ce doping.

The 50Ce-In_2O_3 sensor showed increased τ_{recov} (50 s) compared with the 20Ce-In_2O_3 sensor (47 s) (Fig. 3c). This could be because the agglomeration of 50Ce-In_2O_3particles was more severe than that of 20Ce-In_2O_3 particles by the presence of CeO_2 nanoparticles, resulting in slower gas diffusion. The acetone response of the 50Ce-In_2O_3 sensor was also lower than that of the 20Ce-In_2O_3 sensor, possibly due to the increase in the concentration of Ce and the change in the crystal structure from rhombohedral into cubic. All the facts indicate that the 20 wt% Ce doping is the optimum condition for making In_2O_3 nanoparticle-based sensors highly sensitive and ultrafast to acetone.

To confirm whether the sensor can be used in humid conditions like human breath, we tested the gas-sensing properties of the 20Ce-In_2O_3 sensor under different humidity levels (Fig. 4). Even though the sensor response to 2 ppm acetone constantly decreased with increasing relative humidity (RH) levels, the sensor showed a high acetone response of 4.7 even under RH 60% (Fig. 4a). Moreover, the sensor kept fast response/recovery speeds regardless of RH levels (Fig. 4b). Furthermore, the sensor showed high selectivity to acetone with low cross-responses to other gases, even under RH 60% (Fig. 4c). This demonstrates that the 20Ce-In_2O_3 sensor has high potential in practical application for breath acetone analysis. Accordingly, this sensor can be used

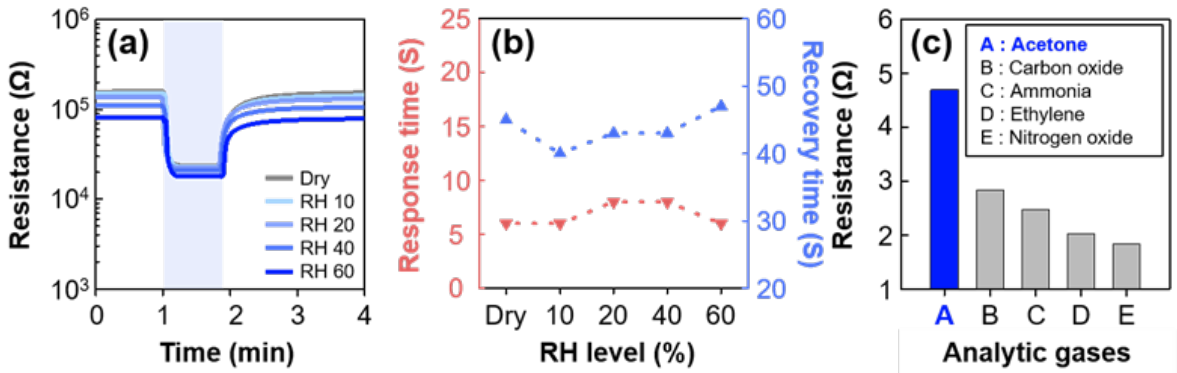

Fig. 4 Gas sensing properties of 20Ce-In_2O_3 sensor at 350 ℃: (a) Gas sensing transients to 2 ppm acetone under different humid conditions (RH 0–60%); (b) response/recovery times upon exposure to 2 ppm acetone under RH 0–60%, (c) Gas response to 2 ppm of acetone, carbon oxide, ammonia, ethylene, and nitrogen oxide under RH 60%.

to realize portable devices for non-invasive fat-burning rate monitoring.

4. Conclusion

We prepared In_2O_3 nanoparticles doped with 0–50 wt% Ce via a one-pot, microwave-assisted hydrothermal method and evaluated their gas-sensing performance with acetone, a breath metabolite of fat burning. While the sensor based on pure In_2O_3 nanoparticles showed a high response and fast response kinetics to acetone, it exhibited slow recovery. As the Ce doping concentration increased from 0 to 20 wt%, both the acetone response and recovery time decreased, while the fast response speed was maintained. This phenomenon was attributed to the increased proportion of Ce with a high oxygen adsorption ability (i.e., gas-insensitive) on the gas-sensing surface of In_2O_3. However, when doped with 50 wt% Ce, the recovery speed slowed again, possibly due to the strong agglomeration of particles caused by the formation of ultrafine CeO_2 nanoparticles. Accordingly, the optimal Ce doping condition was determined to be 20 wt%. Under this condition, the sensor exhibited a sufficiently high acetone response, even though the high amount of gas-insensitive Ce. This was considered to be possible due to the small crystallite size encouraging a large chemo-resistive variation and the gas-sensitive rhombohedral In_2O_3 phase. The In_2O_3sensor doped with 20 wt% Ce demonstrated ultrafast response and recovery speeds, a high response, and good selectivity to acetone, even under humid conditions (RH 0-60%). This suggests that the sensor in the present study can be utilized for breath acetone analysis and non-invasive monitoring of diet efficiency.

Acknowledgement

This work was supported by the R&D program for Forest Science Technology (Project No. "FTIS 201382C10-2221-0101) provided by Korea Forest Service (Korea Forestry Promotion Institute), and Korea Institute of Marine Science & Technology Promotion (KIMST) funded by the Ministry of Oceans and Fisheries (RS-2023-00239826). This work was also carried out with the support of "Cooperative Research Program for Agriculture Science and Technology Development (Project No. PJ016994)" Rural Development Administration, Republic of Korea.

References

[1] H. J. Choi, J. Chung, J. Yoon, J. Lee, Highly selective, sensitive, and rapidly responding acetone sensor using ferroelectric ε-WO_3 spheres doped with Nb for monitoring ketogenic diet efficiency, Sensors and Actuators B: Chemical, 338 (2021) 129823.

[2] K. M. Veloso, S. S. Likhodii, S. C. Cunnane, Breath acetone is a reliable indicator of ketosis in adults consuming ketogenic meals, The American Journal of Clinical Nutrition, 76 (2002) 65-70.

[3] Y. Zhang, L. Zhou, Y. Liu, D. Liu, F. Liu, F. Liu, X. Yan, X. Liang, Y. Gao, G. Lu, Gas sensor based on samarium oxide loaded mulberry-shaped tin oxide for highly selective and sub ppm-level acetone detection, Journal of Colloid and Interface Science, 531 (2018) 74-82.

[4] C. Wang, J. Liu, Q. Yang, P. Sun, Y. Gao, F. Liu, J. Zheng, G. Lu, Ultrasensitive and low detection limit of acetone gas sensor based on W-doped Nio hierarchical nanostructure, Sensors and Actuators B: Chemical, 220 (2015) 59-67.

[5] H. Fan, X. Jia, Selective detection of acetone and gasoline by temperature modulation in zinc oxide nanosheets sensors, Solid State Ionics, 192 (2011) 688-692.

[6] M. I. Ikim, G. N. Gerasimov, B. F. Gromov, O. H. Ilegbusi, L. I. Trakhtenberg, Synthesis, structural and sensor properties of nanosized mixed oxides based on In_2O_3 particles, International Journal of Molecular Sciences, 24 (2023) 1570.

[7] C. Wang, L. Yin, L. Zhang, D. Xiang, R.Gao, Metal oxide gas sensors: sensitivity and influencing factors, Sensors, 10 (2010) 2088-2106.

[8] N. Alizadeh, H. Jamalabadi, F. Tavoli, Breath acetone sensors as non-invasive health monitoring system: a review, IEEE Sensors Journal, 20 (2020) 5-31.

[9] X. Liu, L. Jiang, X. Jiang, X. Tian, X. Sun, Y. Wang, W. He, P. Hou, X. Deng, X. Xu, Synthesis of Ce-doped In_2O_3 nanostructure for gas sensor applications, Applied Surface Science, 428 (2018) 478-484.

[10] M. Karamaoui, S. G. Leonardi, M.Latino, D. M. Tobaldi, N. Donato, R. C. Pullar, M. P. Seabra, J. A. Labrincha, G. Neri, Pt-decorated In_2O_3 nanoparticles and their ability as a highly sensitive (‹10ppb) acetone sensor for biomedical applications, Sensors and Actuators B: Chemical, 230 (2016) 697-705.

[11] J. Yoon, J. Kim, T. Kim, Y. J. Hong, Y.C. Kang, J. Lee, A new strategy for humidity independent oxide chemiresistors: dynamic self-refreshing of In_2O_3 sensing surface assisted by layer-by-layer coated CeO_2 nanoclusters, Small, 12 (2016) 4229-4240.

[12] D. Liu, W. Lei, S. Qin, L. Hou, Z. Liu, Q. Cui, Y. Chen, Large-scale synthesis of hexagonal corundum-type In_2O_3 by ball milling with enhanced lithium storage capabilities, Journal of Materials Chemistry A, 1 (2013) 5274.

[13] M. Sorescu, L. Diamandescu, D. T. Mihaila, V.S. Tedorescu, Nanocrystalline rhombohedral In_2O_3 synthesized by hydrothermal and postannealing pathways, Journal of Materials Science, 39 (2004) 675-677.

[14] T. Liang, D. Kim, J. Yoon, Y. Yu, Rapid synthesis of rhobohedral In_2O_3 nanoparticles via a microwave-assisted hydrothermal pathway and their application for conductometric ethanol sensing, Sensors and Actuators B: Chemical, 346 (2021) 130578.

[15] P. G. Choi, N. Izu, N. Shirahata, Y. Masuda, Improvement of sensing properties for SnO_2 gas sensor by tuning of exposed crystal face, Sensors and Actuators B: Chemical, 296 (2019) 126655.

[16] S. Xia, H. Zhu, H. Cai, J. Zhang, J. Yu, Z. Tang, Hydrothermally synthesized Cuo based volatile organic compound gas sensor, RSC Advances, 4 (2014), 57975.

[17] C. Xu, X. Qu, Cerium oxide nanoparticle: a remarkably versatile rare earth nanomaterial for biological applications, NPG Asia Materials, 6 (2014) e90.